nature biotechnology

Bone marrow–derived stem cells initiate pancreatic regeneration

David Hess[1,6], Li Li[1,6], Matthew Martin[1,2], Seiji Sakano[3], David Hill[2,4], Brenda Strutt[4], Sandra Thyssen[4], Douglas A Gray[5] & Mickie Bhatia[1,2]

We show that transplantation of adult bone marrow–derived cells expressing c-kit reduces hyperglycemia in mice with streptozotocin-induced pancreatic damage. Although quantitative analysis of the pancreas revealed a low frequency of donor insulin-positive cells, these cells were not present at the onset of blood glucose reduction. Instead, the majority of transplanted cells were localized to ductal and islet structures, and their presence was accompanied by a proliferation of recipient pancreatic cells that resulted in insulin production. The capacity of transplanted bone marrow–derived stem cells to initiate endogenous pancreatic tissue regeneration represents a previously unrecognized means by which these cells can contribute to the restoration of organ function.

Bone marrow is an important source of easily procurable adult stem cells[1]. In addition to the ability of bone marrow–derived stem cells to reconstitute the hematopoietic system[1], cells derived from the bone marrow compartment have been shown to possess endothelial[2,3], mesenchymal[4] and pluripotent capabilities[5]. Other recent studies have indicated that transplanted bone marrow–derived stem cells can generate cells with unexpected phenotypes, including muscle[6], liver[7], brain[8] and epithelial lineages[9], suggesting greater developmental plasticity than previously believed[10]. However such events occur at low frequency[11], and the apparent plasticity has been shown in one case to be explained by cellular fusion[12,13]. Despite the obscurity of the cellular mechanism, the ability of transplanted bone marrow to correct physiological function in the whole animal has been documented[7,13,14].

In the context of regenerative therapies, the role of adult stem cells may not be limited to direct replacement of damaged cells. Recent animal and clinical studies have suggested that tissue regeneration can occur upon the introduction of bone marrow–derived stem cells that have multiple effects, including the vascularization of damaged tissue[15]. Vascularization may be facilitated by angiogenic factors released from endothelial cells originating from transplanted bone marrow stem cells[15,16]. In addition, embryonic organogenesis is known to be dependent on tissue-specific endothelium, and endothelial interactions and signaling may play a role in post-natal stem cell engraftment and differentiation[16]. Accordingly, regenerative ability of adult tissue may be directed by essential factors provided by transplanted endothelial cells of bone marrow origin[15,16].

Given the potential therapeutic benefit of bone marrow transplantation, we sought to determine the cellular mechanism and physiological relevance of bone marrow–derived stem cells for the restoration of tissue function after pancreatic injury. Using a mouse model of chemically induced pancreatic damage that causes hyperglycemia, we show that transplantation of bone marrow–derived stem cells initiates endogenous pancreatic regeneration. Engraftment of bone marrow-derived cells to ductal and islet structures was accompanied by rapid proliferation of recipient pancreatic cells and neogenesis of insulin-positive cells of recipient origin.

RESULTS

Model of pancreatic damage and repair

To evaluate the potential capacity of bone marrow–derived stem cells to restore tissue function after injury, we adopted a mouse model of streptozotocin (STZ)-induced pancreatic damage causing hyperglycemia[17] and designed an experimental model to assess pancreatic repair upon transplantation of allogeneic green fluorescent protein (GFP)-expressing bone marrow–derived stem cells (**Fig. 1a**). Recipients were treated daily for 5 d with 35 mg STZ per kg body weight, which induced pancreatic damage (**Fig. 1b**) and secondary hyperglycemia (blood glucose >13.9 mmol/l; **Fig. 1c**). Morphological assessment of pancreatic sections stained with hematoxylin and eosin (H+E) and for insulin showed that pancreatic damage by STZ was associated with the destruction of pancreatic islets at day 10 and a paucity of insulin-expressing cells at day 42 (**Fig. 1b**).

Hyperglycemic mice were intravenously transplanted with transgenic GFP$^+$ bone marrow–derived cells, and blood glucose and serum insulin were monitored (**Fig. 1a**). By day 10 (day of i.v. transplant), blood glucose levels in STZ-treated animals were significantly elevated ($P < 0.05$), and at day 42 blood glucose levels were above 30 mmol/l (**Fig. 1c**). Increased blood glucose correlated with marked reductions in serum insulin by day 10, and these remained attenuated at day 42 as

[1]Robarts Research Institute, Stem Cell Biology and Regenerative Medicine, 100 Perth Drive, London, Ontario N6A 5K8, Canada. [2]The University of Western Ontario, 1151 Richmond Street, London, Ontario N6A 4B8, Canada. [3]Asahi Kasei Corporation, Central R&D and Central Research Laboratory, 2-1 Samajima, Fuji, Shizuoka 416-8501, Japan. [4]Lawson Health Research Institute, 268 Grosvenor Street, London, Ontario N6A 4V2, Canada, and [5]Centre For Cancer Therapeutics, 503 Smyth Road, Ottawa, Ontario K1H 1C4, Canada. [6]These authors contributed equally to this work. Correspondence should be addressed to M.B. (mbhatia@robarts.ca).

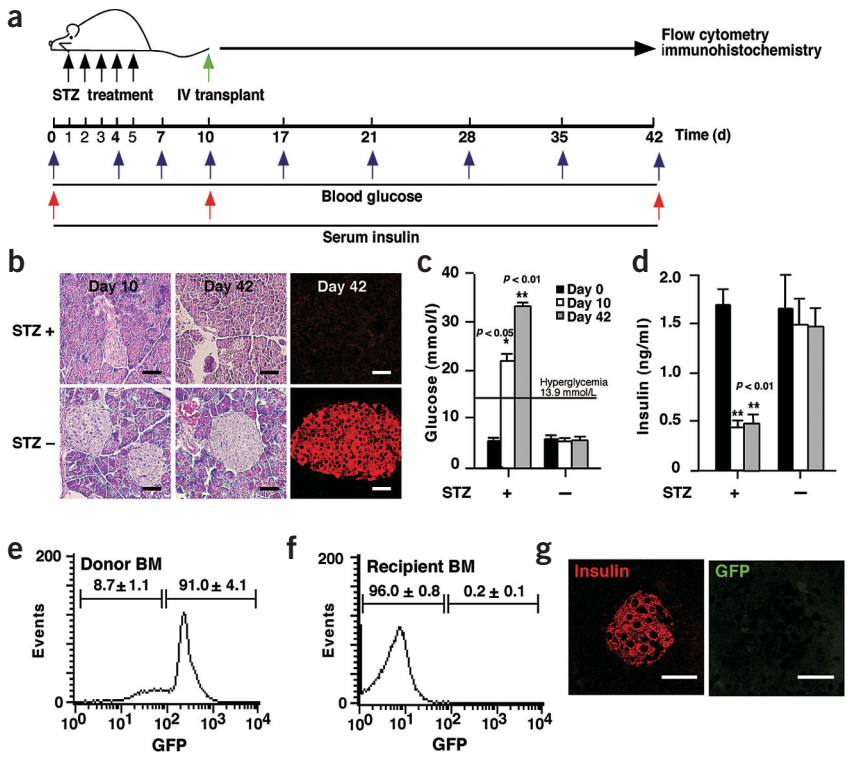

Figure 1 Pancreatic damage and induction of hyperglycemia after STZ treatment in NOD/SCID mice. (**a**) Experimental design for the induction of hyperglycemia and transplantation of GFP$^+$ bone marrow (BM) cells into STZ-treated NOD/SCID mice. (**b**) H+E staining (days 10 and 42) and immunofluorescence (day 42) of pancreatic sections after STZ treatment. As compared to vehicle-treated controls, STZ-treated mice showed fewer islets, altered islet morphology and absence of insulin production. Scale bars, 50 µm. (**c**) i.p. injection of STZ (n = 12) (35 mg/kg/d) or citrate buffer vehicle (n = 9) for 5 d followed by sublethal irradiation (350 cGy) and mock transplantation (PBS) at day 10 resulted in elevated blood glucose from days 10–42. (**d**) Increased blood glucose correlated with decreased systemic insulin measured at days 10 and 42 in STZ-treated mice, in contrast to untreated mice. Data are mean ± s.e.m. (**e**–**g**) Flow cytometry (**e**,**f**) and immunofluorescence assays (**g**) of insulin- and GFP-expressing cells in the BM and pancreas of donor (GFP, n = 4) and non-STZ-treated recipient (NOD/SCID, n = 3) mice. Scale bars, 50 µm.

compared with vehicle-treated controls (**Fig. 1d**). No spontaneous reversion of hypoinsulinemia and hyperglycemia was seen in STZ-treated mice using this protocol. (**Fig. 1c,d**). The absence of mature hematopoietic cells in the pancreas of immune-deficient recipient mice before or after STZ treatment confirmed that pancreatic damage, hypoinsulinemia and secondary hyperglycemia were a result of STZ and were not immune-mediated as previously reported[18,19]. Transplanted bone marrow–derived cells were distinguished from recipient cells by using transgenic donor mice expressing GFP[20]. More than 90% of bone marrow mononuclear cells expressed GFP, as detected by FACS analysis (**Fig. 1e**). In contrast, recipients were devoid of GFP$^+$ cells in the bone marrow (**Fig. 1f**), and ductal and islet regions of pancreatic sections showed no background GFP fluorescence (**Fig. 1g**). This donor-recipient transplantation system established a reproducible model for quantitative measurement of indices of both cellular pancreatic damage and organ function.

Transplantation of bone marrow–derived cells reduces blood glucose

We hypothesized that intravenously transplanted bone marrow–derived cells might improve damaged pancreatic function as evaluated by blood glucose control. Hyperglycemic mice were separated into two groups at day 10: one received PBS control 'transplants' and the other bone marrow–derived cells from GFP donors (**Fig. 2a**). Within 7 d after transplantation (day 17), blood glucose levels were reduced in hyperglycemic mice that had received bone marrow–derived cells. This effect was independent of weight loss or retarded food consumption (data not shown). Blood glucose reduction was sustained from day 17, in contrast to glucose levels in animals that received PBS, which remained severely hyperglycemic and had to be killed (**Fig. 2a**). Mice were also transplanted with GFP$^+$ bone marrow–derived cells that were gamma-irradiated to induce cellular senescence while maintaining survival and the secretion of soluble factors[21]. Mice transplanted with equivalent doses of irradiated GFP$^+$ bone marrow (or tenfold higher; data not shown) remained hyperglycemic (**Fig. 2b**). Based on the similarity of soluble factors released by irradiated vs. nonirradiated bone marrow *in vitro*[21], it is unlikely that soluble factors released from transplanted bone marrow–derived cells are responsible for hyperglycemic reduction.

Neither PBS nor irradiated GFP$^+$ bone marrow transplantation resulted in elevated serum insulin, whereas mice transplanted with GFP$^+$ bone marrow showed a significant increase ($P < 0.01$) in serum insulin concentration (**Fig. 2c**) to levels similar to those in mice devoid of STZ-induced pancreatic damage. At day 42, the beneficial effects were also demonstrated by enhanced survival of bone marrow–transplanted mice as compared to untransplanted STZ-treated mice. Overall, STZ-treated mice that had received bone marrow–derived cell transplants showed a survival rate of 85–75%, in contrast to rates ranging from 50% to as low as 0% survival (100% morbidity) in STZ-treated mice that received PBS. These results indicate that transplantation of bone marrow–derived cells elevates serum insulin and reduces blood glucose levels in hyperglycemic mice with STZ-induced pancreatic tissue damage, thereby improving the metabolic state and survival of recipients.

c-kit$^+$ bone marrow–derived stem cells reduce hyperglycemia

To characterize the bone marrow–derived cells capable of reducing hyperglycemia, we isolated subpopulations based on expression of the stem cell marker c-kit[22,23]. Viable (7-aminoactinomycin D (7-AAD)-excluding) cells were gated and sorted into c-kit$^-$ (R2) and c-kit$^+$ (R1) subsets (**Fig. 2d**) at >98% purity (data not shown), and were transplanted into STZ-treated hyperglycemic mice (**Fig. 2e**). Mice receiving 2×10^6 c-kit$^-$ cells remained hyperglycemic, whereas those receiving 5×10^4 c-kit$^+$ cells (40-fold less than dose of c-kit$^-$ cells) showed reduced blood glucose after day 28 (**Fig. 2e**). The delay in blood glucose reduction with purified c-kit$^+$ cells is reminiscent of delayed tissue reconstitution after transplantation of highly purified stem cells[23,24]. As seen with transplantation of whole bone marrow (**Fig. 2c**), c-kit$^+$ cells increased and sustained serum insulin levels,

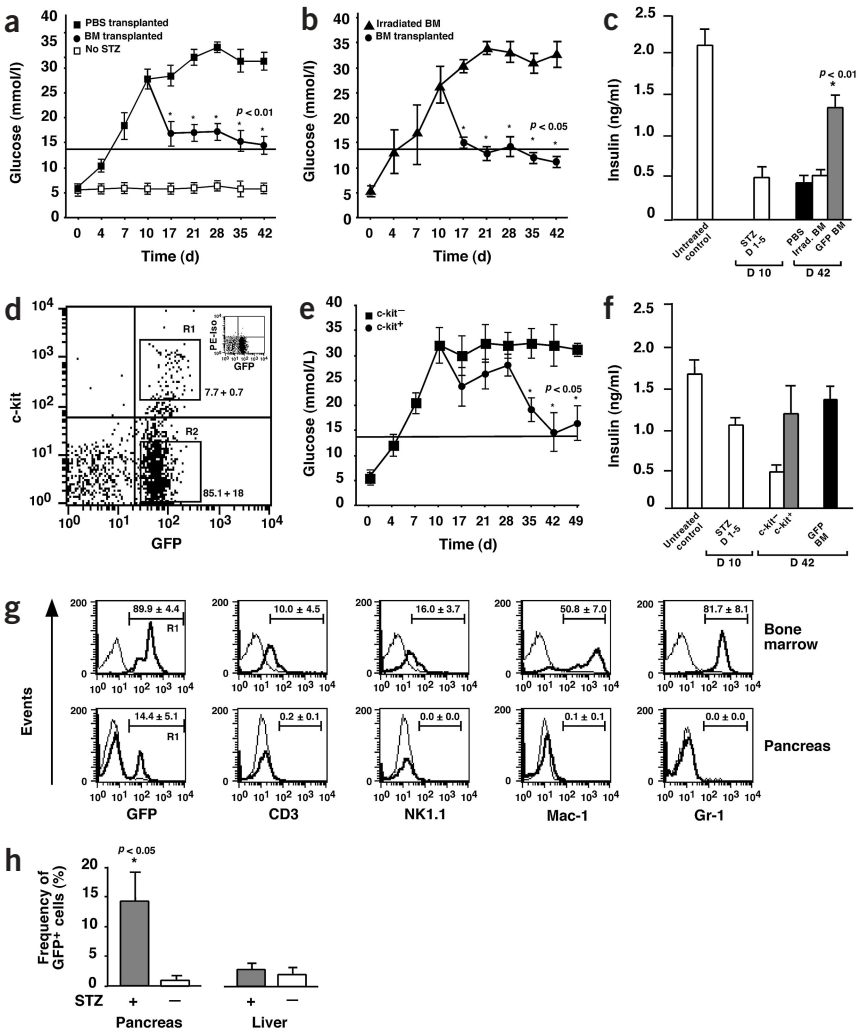

Figure 2 Reduction of elevated blood glucose in STZ-treated NOD/SCID mice after transplantation with functional whole bone marrow (BM) or purified c-kit-expressing BM cells. (**a**,**b**) Comparison of blood glucose in STZ-treated mice injected with PBS (n, $n = 5$) or transplanted with 10^7 GFP$^+$ BM cells (l, $n = 7$) or with 10^7 irradiated GFP$^+$ BM cells (s, $n = 3$). In an independent experiment with three recipients, a more than tenfold greater number of irradiated BM cells was transplanted and similarly had no effect on hyperglycemic recovery (data not shown). Blood glucose in mice not treated with STZ (o, $n = 11$) remained normal. Reduction of elevated blood glucose occurred within 7 d after transplantation of GFP$^+$ BM cells. (**c**) Reduction of blood glucose correlated with increased systemic insulin measured in identical mice. D, day. (**d**) Flow cytometry for the isolation of purified c-kit$^+$ (R1) and c-kit$^-$ (R2) donor BM cells from GFP mice. (**e**) Comparison of blood glucose in STZ-treated mice transplanted with c-kit$^+$ GFP$^+$ BM (l, $n = 6$) or c-kit$^-$ GFP$^+$ BM cells (n, $n = 5$). A range of 50,000–100,000 c-kit$^+$ cells and 100,000–2,000,000 c-kit$^-$ cells were transplanted. Reduction of elevated blood glucose occurred 25 d after the transplant of c-kit$^+$ GFP$^+$ BM cells. Differences in day 10 serum insulin titers between mice transplanted in independent experiments with whole BM (**c**) versus c-kit-selected cells (**f**) were not significant ($P < 0.1$). All comparisons were made within each experimental group; therefore, relative differences between transplanted and untransplanted mice are consistent. (**f**) Reduction of blood glucose correlated with increased systemic insulin measured in identical mice. All glucose and insulin data are shown as mean ± s.e.m. (**g**) Flow cytometric analysis of cells isolated from the BM and pancreas of STZ-treated, NOD/SCID mice transplanted with GFP$^+$ BM cells. GFP$^+$-reconstituting cells in the pancreas were devoid of cells expressing mature hematopoietic markers. Light line, isotype control; dark line, specific antibody. (**h**) Comparisons of the extent of donor chimerism (GFP$^+$ cells) at day 42 between liver and pancreas in individual recipient mice transplanted with BM-derived stem cells. *Significant differences ($P < 0.05$) between distinct groups of transplanted mice.

whereas c-kit$^-$ cells had no effect (**Fig. 2f**). This increase in serum insulin correlated with the reduction in blood glucose (**Fig. 2f**). Reduction of hyperglycemia and hypoinsulinemia was identical in mice transplanted with whole bone marrow and with c-kit$^+$-selected stem cells. Cells derived from c-kit$^+$ bone marrow contributed to chimerism in recipient bone marrow, but also engrafted the damaged pancreas (**Fig. 2g**). Donor-reconstituted (GFP$^+$) mice contained T, NK, macrophage and granulocytic cells in their bone marrow, whereas mature hematopoietic cells were absent in the pancreas despite the presence of an average of 14.4% GFP$^+$ donor-derived bone marrow cells (**Fig. 2g**). Irradiated but non-STZ-treated mice showed similar extent and phenotype of bone marrow chimerism to STZ-treated mice, but fewer than 0.5 ± 0.2% donor GFP$^+$ cells ($n = 11$) in the pancreas as compared to 14.4 ± 5.1% in STZ-treated mice.

We also examined bone marrow engraftment in the liver of STZ-treated and untreated mice (**Fig. 2h**). In the pancreas, mice treated with STZ and transplanted with either c-kit$^+$ or whole bone marrow showed 14.4 ± 5.1% chimerism, as compared to only 1.0 ± 0.7% chimerism seen in mice not treated with STZ ($P < 0.05$). In contrast, liver chimerism in STZ-treated recipients was not significantly different from liver chimerism in untreated recipients (2.8 ± 1.0% versus 1.8 ± 1.2%, respectively ($P < 0.1$)) or to chimerism in the pancreata of untreated recipients (**Fig. 2h**). These results indicate that bone marrow–derived stem cells preferentially engraft damaged pancreatic tissue as compared with undamaged pancreas and the liver of STZ-treated and -untreated animals, further supporting the notion that tissue damage is necessary for the recruitment of bone marrow–derived cells. We suggest that bone marrow–derived c-kit$^+$ cells are responsible for recovery of insulin and glucose control in STZ-treated mice.

Bone marrow–derived stem cells engraft pancreatic structures

To characterize pancreatic engraftment, we performed immunohistochemical analysis of tissue sections. As illustrated by H+E staining, donor GFP$^+$ cells were detected in two regions, the ductal and islet sites (**Fig. 3a**). Costaining for insulin showed that the majority of bone marrow–derived GFP$^+$ cells were devoid of insulin; however, a small proportion of donor bone marrow–derived (GFP$^+$) cells surrounding islet structures stained positive for insulin (arrow, **Fig. 3a**). We next analyzed individual cells to further characterize insulin-positive bone marrow–derived cells. Subcellular localization of GFP

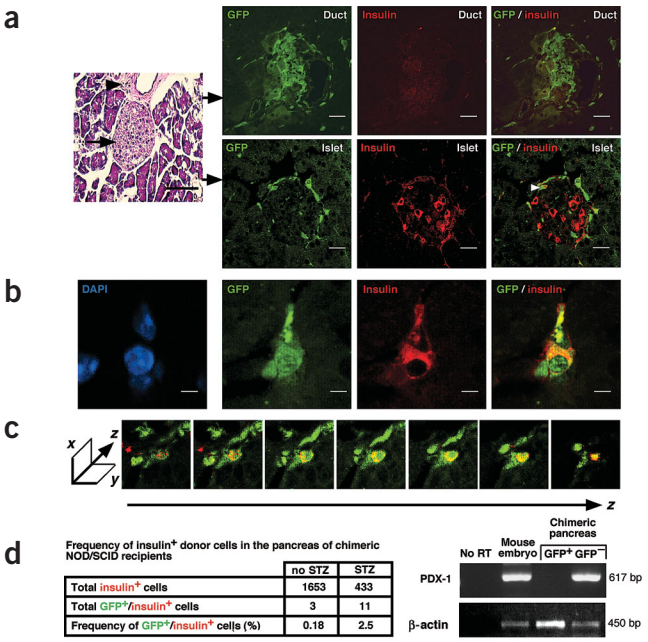

Figure 3 Transplanted donor bone marrow (BM) cells engraft ductal and islet regions in recipient pancreas and produce a low frequency of donor insulin-positive (insulin$^+$) cells devoid of PDX-1 expression. (**a**) GFP and insulin expression of donor cells engrafting the ductal epithelial region and surrounding recipient-derived insulin producing cells. White arrowheads indicate insulin-producing donor cells in the ductal (black arrowhead, top left) and islet (black arrow, middle left) regions. Scale bars, 50 μm. (**b**) Visualization of insulin-producing donor (insulin$^+$, GFP$^+$) cell. Scale bars, 10 μm. (**c**) *z*-series of a single insulin-producing donor cell. Cytoplasmic staining of insulin granules with GFP expression was observed throughout the nuclear and cytoplasmic regions. Each panel represents serial images (5 μm) through the thickness of the tissue. (**d**) Frequency of insulin-producing donor cells in the pancreas of NOD/SCID recipients. (**e**) RT-PCR showing PDX-1 mRNA levels in donor and recipient cells in the pancreas of NOD/SCID recipients; β-actin mRNA was assessed as input template control. Data are shown as mean ± s.e.m. Tissue sectioning analysis was performed as detailed in methods.

was observed in both nuclear and cytoplasmic compartments, whereas insulin was found exclusively in the cytoplasm and not in 4,6-diamidino-2-phenylindole (DAPI)-stained nuclei (blue, **Fig. 3b**). Incremental *z*-series images indicated that single GFP$^+$, insulin-positive cells could be dissected to reveal cellular localization of insulin that followed a punctate cytoplasmic pattern (**Fig. 3c**).

We compared the frequency of donor GFP$^+$ bone marrow–derived cells coexpressing insulin in STZ-treated and vehicle-treated recipients (**Fig. 3d**). Among mice transplanted with GFP$^+$ bone marrow–derived cells, GFP$^+$ insulin-positive cells (cells of donor origin) were nearly absent in the pancreas of non-STZ-treated mice but made up 2.5% of insulin-positive cells in the pancreas of STZ-treated animals. The presence of insulin-positive donor cells only in STZ-treated mice suggests that pancreatic damage was required for this phenotype to be observed.

Because embryonic stem cells have demonstrated immunoreactivity to insulin resulting from the uptake of exogenous insulin available *in vitro*[25], we sought to determine whether observable insulin-positive, donor bone marrow–derived cells expressed PDX-1, a transcription factor that binds to the insulin promoter and is essential for glucose-stimulated insulin production[26,27]. Donor GFP$^+$ and endogenous GFP$^-$ cells were isolated from pancreatic tissues and analyzed for PDX-1 expression by RT-PCR. Recipient GFP$^-$ pancreatic cells expressed PDX-1, whereas donor GFP$^+$ cells derived from the bone marrow did not (**Fig. 3e**). Thus, although bone marrow–derived cells were capable of adopting a β-cell phenotype (insulin positive), they did not express a molecular factor associated with β-cell development[28].

Based on the inability to demonstrate significant insulin production from transplanted bone marrow–derived cells, we postulate that endogenous pancreatic cells of the recipient may be primarily responsible for amelioration of hyperglycemia in our model.

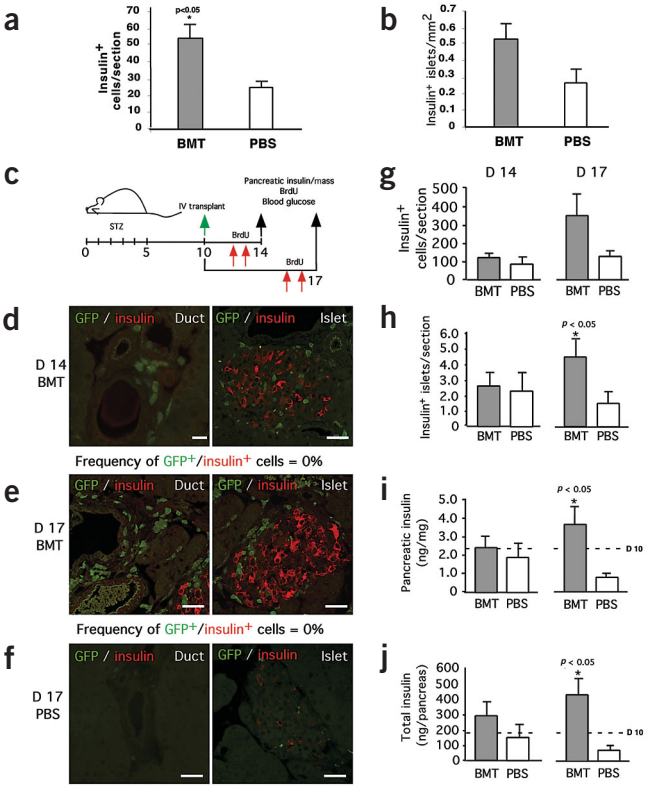

Figure 4 Donor bone marrow–derived stem cells rapidly engraft the pancreas of recipient mice and induce endogenous pancreatic insulin production. (**a**,**b**) Analysis of the number of insulin-positive cells per section and the number of islets per mm^2 in the pancreas of STZ-treated NOD/SCID recipients at day 42. BMT, bone marrow transplant. (**c**) Experimental design for the detection of insulin-producing cells, PECAM-1-expressing donor cells and BrdU-labeled proliferating cells in the pancreases of hyperglycemic mice 4 and 7 d after transplant with GFP$^+$ bone marrow (BM) cells or mock transplanted with PBS. (**d**–**f**) Representative analysis of GFP and insulin expressing cells detected in pancreatic ductal and islets regions at 4 (day 14 (D 14)) and 7 days (day 17 (D 17)) after intravenous (IV) transplantation of either BM or PBS. (**g**,**h**) Quantitative analysis of the number of insulin-producing cells (**g**) and the number of islet structures per section (**h**) in the pancreas of STZ-treated mice, 4 and 7 d after transplantation with either BM or PBS. (**i**,**j**) Quantitative analysis of the pancreatic mass (**i**) and total pancreatic insulin content (**j**) in STZ-treated mice 4 and 7 d after BM transplant or PBS injection. Horizontal dotted line indicates levels at day 10 before transplantation. All data are mean ± s.e.m. ($n = 5$ mice per group). A significant ($P < 0.05$) increase in pancreas insulin content was observed in BM transplanted mice within 7 d. Horizontal dotted line indicates levels at d 10 before transplantation.

Bone marrow–derived stem cells initiate endogenous insulin production

To investigate the role of endogenous β-cells in our model, we compared the total number of insulin-positive cells in the pancreases of transplanted mice treated with STZ, irrespective of donor or recipient origin. At day 42, the total number of insulin-positive cells per section (**Fig. 4a**) and the number of insulin-positive islets (**Fig. 4b**, expressed per mm^2) were greater in mice transplanted with GFP^+ bone marrow than mice transplanted with PBS or irradiated GFP^+ bone marrow (**Fig. 2a,b**). Because transplantation of donor bone marrow produced rapid reduction of elevated blood glucose within 7 d (**Fig. 2a,b**) and an increase in insulin-positive islets, we aimed to characterize the relationship between donor cell engraftment in pancreas and initiation of hyperglycemic reduction.

We analyzed donor cell engraftment and insulin production in the pancreases of STZ-treated hyperglycemic mice transplanted with either unpurified bone marrow–derived cells or PBS during the onset of blood glucose reduction at day 14–17 (**Fig. 4c**). As early as 4 d after bone marrow transplantation (day 14), donor GFP^+ cells could be detected in surrounding pancreatic duct and islets sites (**Fig. 4d**). Very few insulin-expressing cells were observed in islets and none in ductal regions (**Fig. 4d**). At day 17, duct and islet structures were surrounded by greater numbers of bone marrow–derived donor cells (**Fig. 4e**). Islet structures in bone marrow–transplanted mice also contained more insulin-producing cells by day 17 (**Fig. 4e**), in contrast to STZ-treated mice transplanted with PBS, which contained few islets and only residual insulin-expressing cells (**Fig. 4f**). Insulin-positive bone marrow–derived cells (GFP^+, insulin-positive cells) were not detected at either day 14 or day 17 (**Fig. 4d,e**). The absence of GFP^+, insulin-positive cells during the initial stages of blood glucose reduction further emphasizes that bone marrow–derived cells did not directly contribute to insulin production and restoration of glucose control.

Substantial numbers of insulin-producing islets were observed by day 17 in mice transplanted with bone marrow (**Fig. 4g,h**), consistent with direct measurement of pancreatic insulin content (**Fig. 4i,j**). At day 14, pancreatic insulin levels were similar in bone marrow–transplanted and PBS-treated control mice. By day 17, however, mice that had received bone marrow transplants showed marked increases in insulin (**Fig. 4i,j**), correlating with significant reductions ($P < 0.001$) in blood glucose levels (16.5 ± 1.1 mmol/l (mean ± s.e.m.), $n = 7$), whereas PBS-transplanted control mice remained hyperglycemic (29.8 ± 1.2 mmol/l, $n = 6$). These results indicate that transplantation of bone marrow–derived stem cells is accompanied by a rapid increase in endogenous sources of pancreatic insulin and a reduction in blood glucose levels.

Proliferative regeneration initiated by bone marrow–derived stem cells

On the basis of our observations, we surmised that substantial proliferation of the pancreases of bone marrow–transplanted recipients would be required to establish newly generated cells. To assess this, hyperglycemic mice transplanted at day 10 with either bone marrow or PBS were given two single injections of BrdU at 50 μg/kg body weight and killed at day 14 or day 17 for analysis (**Fig. 4c**).

To establish the normal homeostatic turnover of pancreatic cells, we injected untreated recipient mice with BrdU and examined them for proliferating cells (**Fig. 5a**). Unlike tissue known to undergo continual renewal, such as testis and intestine, undamaged pancreas of normoglycemic mice contained nearly undetectable numbers of proliferating ($BrdU^+$) cells (**Fig. 5a**), suggestive of a low frequency of

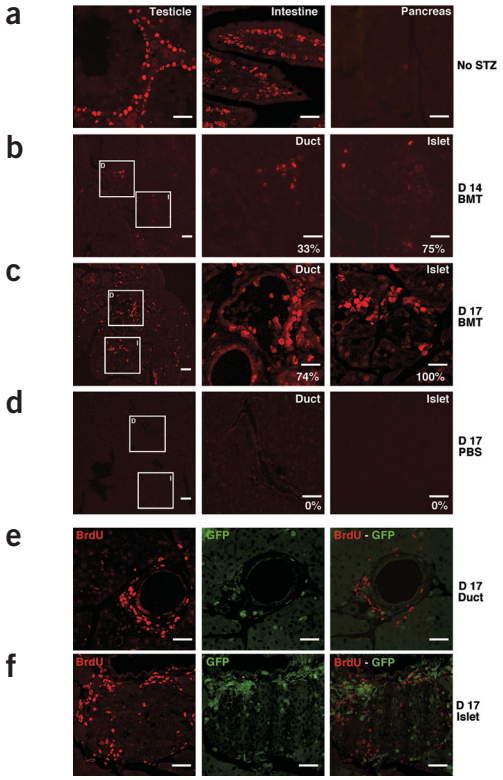

Figure 5 GFP^+ donor cells in the pancreas of transplanted recipient mice promote the proliferation of cells in the ductal and pancreatic islet regions. (**a**) Visualization of BrdU-labeled proliferating cells in the testicle, intestine and pancreas of NOD/SCID mice not injected with STZ. (**b**–**d**) Visualization of BrdU-labeled proliferating cells in the ductal (D) and islet (I) regions of the pancreas of STZ-treated mice, 4 and 7 d after bone marrow (BMT) or PBS transplantation. (**e**,**f**) Serial 5 μM pancreatic sections were stained for BrdU and, after section, used for detection of GFP. Sequential sections were then superimposed to distinguish recipient- versus donor-derived proliferating cells in the ductal and islet pancreatic structures. Simultaneous BrdU and GFP detection could not be visualized on a single section because the acid treatment required to denature DNA for BrdU detection destroys fluorescent properties of GFP, resulting in false-positive artifacts (data not shown). Scale bars, 50 μm.

cellular turnover. In contrast, by day 14 the pancreases of STZ-induced hyperglycemic mice transplanted with bone marrow–derived cells contained $BrdU^+$ cells in both ductal and islet sites, whose numbers increased by day 17 (**Fig. 5b,c**). The proportion of total ductal and islet structures containing more than two proliferating cells was quantified (**Fig. 5b,c**). At day 14, only 33% of ductal structures contained cells undergoing division, whereas 75% of islet structures contained proliferating cells (**Fig. 5b**). By day 17 the proportion of proliferating ductal sites increased to 74%, and all islet structures contained proliferation cells (**Fig. 5c**). Without transplantation of bone marrow–derived cells, no proliferation was detected in ductal and islet structures of STZ-treated mice that had received PBS (**Fig. 5d**).

To distinguish donor bone marrow–derived cells from recipient pancreatic cells, we stained sequential serial sections of ductal and islet tissue for BrdU and donor-derived GFP^+ cells. Of the proliferating ($BrdU^+$) cells surrounding the pancreatic ductal regions of bone marrow–transplanted mice, the majority did not colocalize with GFP^+ donor cells, as determined by comparison of sequential sections and by identification of $BrdU^+$, GFP^+ (yellow) cells upon superimposition

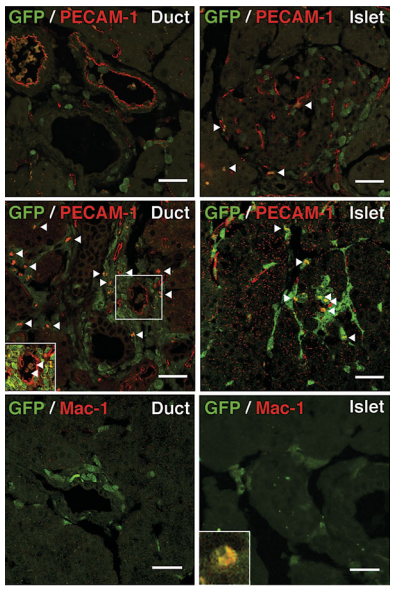

d

Frequency of PECAM-1$^+$ endothelial cells in the pancreas of NOD/SCID recipients

	No STZ	STZ
Frequency of PECAM-1$^+$ cells (cells/μm^2)	10.1	21.3
Total GFP$^+$ cells	177	316
Total GFP$^+$/PECAM-1$^+$ cells	1	29
Frequency GFP$^+$/PECAM-1$^+$ cells (%)	0.6	9.2

Figure 6 Pancreatic engraftment of donor-derived PECAM-1$^+$ endothelial cells correlates with the rapid reduction of hyperglycemia after transplant. (**a**,**b**) Representative analysis of PECAM-1-expressing GFP$^+$ donor cells surrounding pancreatic duct and islet structures of recipient NOD/SCID mice at day 17 and day 42. Arrowheads indicate double-stained GFP$^+$/PECAM-1$^+$ cells. For quantitative analysis, red blood cells showing autofluorescence were excluded. A representative artifact of this kind that was deliberately excluded from our analysis is shown in the inset (arrows indicate false-positive 'yellow' red blood cells). Scale bars, 50 μm. (**c**) GFP$^+$ donor cells surrounding pancreatic duct and islet structures of recipient NOD/SCID mice do not coexpress the monocyte and macrophage marker MAC-1. (**d**) Frequency of PECAM-1$^+$ endothelial cells in the chimeric pancreas of NOD/SCID recipients at day 42 with or without STZ treatment. Frequency of endothelial cells, independent of donor or recipient origin, is shown as cells per μm^2 and was higher in transplanted mice treated with STZ ($P < 0.005$). Tissue sectioning analysis (detailed in Methods) also demonstrated that blood vessel number was not increased in the transplanted recipient pancreas as assessed by morphological examination of H+E-stained pancreatic sections (data not shown), indicating that angiogenesis did not contribute to pancreatic regeneration.

of serial images (**Fig. 5e**). Proliferating BrdU$^+$ cells in the islet regions also included few BrdU$^+$, GFP$^+$ bone marrow–derived donor cells (**Fig. 5f**). These analyses indicated that the majority of proliferating cells in the ductal and islet regions were of recipient pancreatic origin.

Potential role of bone marrow–derived endothelial cells

Inspired by recent evidence indicating that endothelial interaction is critical for pancreatic β–cell development[29], we examined the pancreases of transplanted mice for endothelial cells. Pancreatic sections from mice that sustained reduction in blood glucose as a result of transplantation of bone marrow–derived stem cells were also analyzed at days 17 and 42 for donor and PECAM-1$^+$ cells (**Fig. 6**). Donor-derived endothelial (GFP$^+$ PECAM-1$^+$) cells were detected in islet regions 7 d after transplantation (**Fig. 6a**, arrows). Increased numbers of donor-derived endothelial cells were also seen in ductal and islet regions at day 42. In addition, immunostaining of pancreas sections stained with macrophage-specific antibody (MAC-1) showed that all sections were devoid of MAC-1$^+$ donor cells (**Fig. 6c**). The number of bone marrow–derived endothelial (GFP$^+$ PECAM-1$^+$) cells detected in mice transplanted with bone marrow–derived cells was compared in recipients treated with STZ and with vehicle (**Fig. 6d**). As many as 9.2% of donor bone marrow–derived cells engrafting ductal or islet regions were of endothelial lineage (GFP$^+$ PECAM-1$^+$), whereas non-STZ-treated transplanted mice were devoid of donor endothelial cells, suggesting that pancreatic injury was required for the recruitment of bone marrow donor endothelial cells. Independent of donor origin, the number of endothelial cells was significantly higher ($P < 0.005$) in bone marrow–transplanted mice treated with STZ (**Fig. 6d**), suggesting that endothelial interactions may also involve contributing effects of recipient pancreatic endothelium. In line with previous observations of pancreatic neogenesis during embryonic development[30], we suggest that a similar regenerative process can be initiated in the adult by transplantation of bone marrow–derived stem cells that give rise to mature donor endothelial cells.

DISCUSSION

Our results indicate that pancreatic engrafting cells derived from donor bone marrow cells can reverse hypoinsulinemia and hyperglycemia caused by pancreatic damage. Although insulin-positive, bone marrow–derived cells were present in sections of STZ-damaged pancreatic tissue, the complete absence of these cells during the onset of hyperglycemic reduction, their low frequency, and our inability to detect the transcription factor PDX-1 (ref. 26) suggested that the bone marrow–derived cells did not, in themselves, functionally rescue the recipients.

Transplantation initiated proliferation of the pancreatic cells within 7 d, and was accompanied by increases in insulin-expressing cells, islet structures, and pancreatic and serum insulin production that resulted in control of blood glucose. Analogous regenerative processes have been reported in such organisms as salamanders and *Caenorhabditis elegans*. More recently, neural stem cell transplantation was shown to 'rescue' dysfunctional recipient neurons in brain tissue damaged by hypoxic-ischemic injury[31,32].

The mechanism by which bone marrow–derived stem cells induce endogenous pancreatic tissue repair is not yet known. However, the rapidity of the regeneration process and of the emergence of proliferating pancreatic cells suggests that endogenous pancreatic stem cells may mediate the restorative process through endothelial interactions[33,34,35]. Bone marrow transplantation may be a feasible approach to managing patients with pancreatic damage, such as that found in type II diabetics[36] and might extend to the regeneration of other organs and tissues.

METHODS

Induction of hyperglycemia, blood glucose monitoring and BrdU injections. Immune-deficient NOD/SCID mice (Jackson Laboratories) 8–10 weeks of age were injected intraperitoneally (i.p.) with 35 mg/kg STZ (Sigma-Aldrich) daily for days 1–5. STZ was solubilized in sodium citrate buffer, pH 4.5, and injected within 15 min of preparation. Blood glucose was measured between 8:00 and 10:00 AM, twice weekly from day 0 to day 14 and weekly from day 14 to day 49, with a glucometer Elite diabetes care system (Bayer). Peripheral blood (100 μl) was collected on days 0, 10 and 42, and serum insulin was quantified with a ^{125}I-labeled, mouse insulin–specific radioimmunoassay (Linco). For the *in vivo* detection of proliferating cells in the pancreas of recipient NOD/SCID mice, BrdU (50 μg/kg body weight in PBS; Sigma) was injected i.p. 16 and 2 h before pancreas extraction. NOD/SCID mice were maintained under sterile conditions in microisolator cages in ventilated racks with treatment and

transplantation protocols approved by local animal care and ethics committees of the Robarts Research Institute and the University of Western Ontario.

Transplantation of hyperglycemic mice. Bone marrow cells from GFP-expressing transgenic Friend leukemia virus B mice[20] were extracted from the tibias, femurs, and iliac crest and transplanted by tail-vein injection into sublethally irradiated (350 cGy) STZ-treated or vehicle-treated NOD/SCID mice. GFP^+ bone marrow cells (10^6) were transplanted *de novo* or irradiated (1,500 cGy) before transplant to arrest their proliferative capacity. GFP-expressing c-kit^- and c-kit^+ (10^5) cells were purified by staining with anti-CD117–APC (allophycocyanin) (c-kit) antibody (Becton Dickinson (BD)), and sorted with a fluorescence-activated cell sorter (FACSVantage SE) and CellQuest software (BD). Sorting gates were established on GFP^+ bone marrow cells stained with fluorochrome-conjugated IgG_1 as isotype (BD). c-kit^+ and c-kit^- cells were also plated into Methocult GF M3434 semisolid media (Stem Cell Technologies) and were assayed for *in vitro* clonogenic progenitor capacity as described previously[37]. Colony formation was enumerated by light microscopy after 14 d, and showed >100-fold enrichment in clonogenic progenitors in the c-kit^+ fraction compared to c-kit^- cells.

Flow cytometry of mouse bone marrow and pancreas. Bone marrow cells were harvested from the tibiae, femurs, and iliac crest of transplanted mice, and the proximal portion of each pancreas was harvested and mechanically separated into a single cell suspension without protease digestion. Approximately 10^6 bone marrow or pancreas cells were stained with the viability dye 7-AAD (Beckman Coulter) and analyzed for the presence of GFP-expressing donor cells on a FACSCalibur cytometer (BD). For multilineage analysis of hematopoietic and endothelial cell surface markers, bone marrow or pancreas cells from transplanted mice were incubated with mouse anti-CD3–phycoerythrin (anti-CD3–PE), anti-NK1.1–PE, anti-Mac-PE, anti-Gr-1–PE, anti–PECAM-1–PE or isotype-matched controls (all antibodies from BD), and analyzed after gating for GFP^+ donor cells.

Pancreatic insulin. A portion of each pancreas was isolated for quantification of total insulin content. Insulin was extracted by mechanical homogenization in the presence of 1 ml acid ethanol (165 mM HCl in 75% ethanol). After 18 h of incubation at 4 °C, insulin was quantified in the supernatant by radioimmunoassay (Linco) and normalized per milligram pancreatic tissue[38].

Immunohistochemistry. The distal portion of each pancreas was fixed overnight in 10% (buffered formalin, incubated with 30% sucrose in 0.1 M PBS at 4 °C, and embedded in frozen tissue embedding gel (Fisher). Serial sagittal cryosections were cut at a thickness of 5 μm and spanned approximately 760 μm of the distal region of the pancreas. Three individual sections per animal, separated by 180 μm, were selected for each immunostaining analysis. Sections were immunostained with mouse anti-insulin (1:2,000, Sigma), rat anti–PECAM-1 (CD31; 1:20; BD), rabbit anti–Mac-1 (CD11b; 1:10; BD), mouse anti-BrdU (1:50; Dako), or isotype-matched control antibodies. For BrdU staining, cryosections were pretreated with 3 N HCl for 30 min at 37 °C to denature DNA. Labeled cells were visualized with a biotin-conjugated secondary antibody with a streptavidin–Texas red system (Vector Laboratories). Isotype-matched antibodies and PBS were used as controls for stained sections. Nuclear regions were stained by DAPI counterstaining (Vector). Images were collected with an Olympus confocal laser-scanning microscope. Tissue sectioning and analysis shown is based on 6–12 mice per group. For a given product indicated in the figures, 30 pancreatic sections were isolated per mouse pancreas, and a minimum of 3 sections per mouse were blindly analyzed the from 1st, 10th and 20th sections to derive an average and s.e.m. used to draw conclusions. For each treatment group, the data from each mouse were then pooled to calculate the overall mean shown. When analyzed individually, all mice within a given group demonstrated results consistent results with the overall average shown.

Histomorphometry. Three sections per animal were stained with H+E to allow assessment of pancreatic islet morphology after STZ treatment and subsequent transplantation. Islet size and number were scored with an Olympus light microscope IX50 and a computer-assisted image analysis program (Image Pro Plus 4.5).

RT-PCR. Unprocessed cells from the pancreas of chimeric mice were sorted for GFP^+ (donor) and GFP^- (recipient) cells with a FACSVantage SE cytometer, and flash-frozen in liquid nitrogen. mRNA was extracted with a QuickPrep micro mRNA purification kit and cDNA was synthesized with a First-Strand cDNA synthesis kit (Amersham Pharmacia). PDX-1-specific sequences were amplified by PCR (Gene Amp PCR System 9700, Perkin Elmer) with the following primers: PDX-1-Forward, 5′-CCA CAC AGC TCT ACA AGG ACC-3′; PDX-1-Reverse, 5′-CGT TGT CCC GCT ACT ACG TTT C-3′; β-actin-P1, 5′-GATCCACATCTGCTGGAAGG-3′; and β-actin-P2, 5′-AAGTGACGTTGACATCCG-3′.

Statistics. Blood glucose and serum insulin concentrations were shown as the mean ± s.e.m. for mice grouped by transplanted cell populations or mock (PBS) injection. Statistical analysis for significance was done with a two-tailed Student's *t*-test.

ACKNOWLEDGMENTS

Funding for this research project was provided by the Canadian Institutes of Health Research, Asahi Kasei Corporation, and a fellowship award from the CIHR for D.H., and a Canadian Research Chair in Stem Cell Biology and Regenerative Medicine to M.B. Special thanks to Krysta Levac, Lisheng Wang, Francis Karanu, Julie McBride and Kristin Chadwick for their insights and assistance towards this work.

COMPETING INTERESTS STATEMENT

The authors declare that they have no competing financial interests.

Received 10 February; accepted 1 May 2003
Published online 22 June 2003; doi:10.1038/nbt841

1. Weissman, I.L., Sander, M. & German, M.S. Stem cells: units of development, units of regeneration, and units in evolution. *Cell* **100**, 157–168 (2000).
2. Hattori, K. *et al.* Placental growth factor reconstitutes hematopoiesis by recruiting $VEGFR1^+$ stem cells from bone-marrow microenvironment. *Nat. Med.* **8**, 841–849 (2002).
3. Verfaillie, C.M. Adult stem cells: assessing the case for pluripotency. *Trends Cell Biol.* **12**, 502–508 (2002).
4. Pittenger, M.F., Mosca, J.D. & McIntosh, K.R. Human mesenchymal stem cells: progenitor cells for cartilage, bone, fat and stroma. *Curr. Top. Microbiol. Immunol.* **251**, 3–11 (2000).
5. Jiang, Y. *et al.* Pluripotency of mesenchymal stem cells derived from adult marrow. *Nature* **418**, 41–49 (2002).
6. Jackson, K.A., Mi, T. & Goodell, M.A. Hematopoietic potential of stem cells isolated from murine skeletal muscle. *Proc. Natl. Acad. Sci. USA* **96**, 14482–14486 (1999).
7. Lagasse, E. *et al.* Purified hematopoietic stem cells can differentiate into hepatocytes *in vivo*. *Nat. Med.* **6**, 1229–1234 (2000).
8. Brazelton, T.R., Rossi, F.M., Keshet, G.I. & Blau, H.M. From marrow to brain: expression of neuronal phenotypes in adult mice. *Science* **290**, 1775–1779 (2000).
9. Krause, D.S. *et al.* Multi-organ, multi-lineage engraftment by a single bone marrow-derived stem cell. *Cell* **105**, 369–377 (2001).
10. Springer, M.L., Brazelton, T.R., Blau, H.M., Rossi, F.M. & Keshet, G.I. Not the usual suspects: the unexpected sources of tissue regeneration. *J. Clin. Invest.* **107**, 1355–1356 (2001).
11. Wagers, A.J., Sherwood, R.I., Christensen, J.L. & Weissman, I.L. Little evidence for developmental plasticity of adult hematopoietic stem cells. *Science* **297**, 2256–2259 (2002).
12. Wang, X. *et al.* Cell fusion is the principal source of bone-marrow-derived hepatocytes. *Nature* **422**, 897–901 (2003).
13. Vassilopoulos, G., Wang, P.R. & Russell, D.W. Transplanted bone marrow regenerates liver by cell fusion. *Nature* **422**, 901–904 (2003).
14. Orlic, D. *et al.* Bone marrow cells regenerate infarcted myocardium. *Nature* **410**, 701–705 (2001).
15. Raffii, S. & Lyden, D. Therapeutic stem and progenitor cell transplantation for organ vascularization and regeneration. *Nat. Med.* **9**, 702–712 (2003).
16. Cleaver, O. & Melton, D. Endothelial signaling during development. *Nat. Med.* **9**, 661–668 (2003).
17. Zysset, T. & Sommer, L. Diabetes alters drug metabolism—*in vivo* studies in a streptozotozin-diabetic rat model. *Experientia* **42**, 560–562 (1986).
18. Gerling, I.C., Friedman, H., Greiner, D.L., Shultz, L.D. & Leiter, E.H. Multiple low-dose streptozocin-induced diabetes in NOD-scid/scid mice in the absence of functional lymphocytes. *Diabetes* **43**, 433–440 (1994).
19. Elliott, J.I., Dewchand, H. & Altmann, D.M. Streptozotocin-induced diabetes in mice lacking αβ T cells. *Clin. Exp. Immunol.* **109**, 116–120 (1997).
20. Tsirigotis, M. *et al.* Analysis of ubiquitination *in vivo* using a transgenic mouse model. *Biotechniques* **31**, 120–126 (2001).
21. Quesenberry, P. *et al.* Studies on the regulation of hemopoiesis. *Exp. Hematol.* **13**, 43–48 (1985).
22. Nakauchi, H., Sudo, K. & Ema, H. Quantitative assessment of the stem cell self-

renewal capacity. *Ann. N.Y. Acad. Sci.* **938**, 18–24 (2001).
23. Ortiz, M. *et al.* Functional characterization of a novel hematopoietic stem cell and its place in the c-Kit maturation pathway in bone marrow cell development. *Immunity* **10**, 173–182 (1999).
24. Tsai, R.Y. *et al.* Plasticity, niches, and the use of stem cells. *Dev. Cell* **2**, 707–712 (2002).
25. Rajagopal, J., Anderson, W.J., Kume, S., Martinez, O.I. & Melton, D.A. Insulin staining of ES cell progeny from insulin uptake. *Science* **299**, 363 (2003).
26. Offield, M.F. *et al.* PDX-1 is required for pancreatic outgrowth and differentiation of the rostral duodenum. *Development* **122**, 983–995 (1996).
27. Shih, D.Q. *et al.* Profound defects in pancreatic β-cell function in mice with combined heterozygous mutations in Pdx-1, Hnf-1α, and Hnf-3β. *Proc. Natl. Acad. Sci. USA* **99**, 3818–3823 (2002).
28. Sander, M. & German, M.S. The β cell transcription factors and development of the pancreas. *J. Mol. Med.* **75**, 327–340 (1997).
29. Lammert, E., Cleaver, O. & Melton, D. Induction of pancreatic differentiation by signals from blood vessels. *Science* **294**, 564–567 (2001).
30. Lammert, E., Cleaver, O. & Melton, D. Role of endothelial cells in early pancreas and liver development. *Mech. Dev.* **120**, 59–64 (2003).
31. Park, K.I., Teng, Y.D. & Snyder, E.Y. The injured brain interacts reciprocally with neural stem cells supported by scaffolds to reconstitute lost tissue. *Nat. Biotechnol.* **20**, 1111–1117 (2002).
32. Ourednik, J., Ourednik, V., Lynch, W.P., Schachner, M. & Snyder, E.Y. Neural stem cells display an inherent mechanism for rescuing dysfunctional neurons. *Nat. Biotechnol.* **20**, 1103–1110 (2002).
33. Edlund, H. Pancreatic organogenesis—developmental mechanisms and implications for therapy. *Nat. Rev. Genet.* **3**, 524–532 (2002).
34. Peters, J., Jurgensen, A. & Kloppel, G. Ontogeny, differentiation and growth of the endocrine pancreas. *Virchows Arch.* **436**, 527–538 (2000).
35. Zulewski, H. *et al.* Multipotential nestin-positive stem cells isolated from adult pancreatic islets differentiate *ex vivo* into pancreatic endocrine, exocrine, and hepatic phenotypes. *Diabetes* **50**, 521–533 (2001).
36. Haluzik, M. & Nedvidkova, J. The role of nitric oxide in the development of streptozotocin-induced diabetes mellitus: experimental and clinical implications. *Physiol. Res.* **49**, S37–42 (2000).
37. Bhardwaj, G. *et al.* Sonic hedgehog induces the proliferation of primitive human hematopoietic cells via BMP regulation. *Nat. Immunol.* **2**, 172–180 (2001).
38. Burkart, V. *et al.* Mice lacking the poly(ADP-ribose) polymerase gene are resistant to pancreatic β-cell destruction and diabetes development induced by streptozocin. *Nat. Med.* **5**, 314–319 (1999).